

Belief Propagation-based Rotation and Translation Estimation for Rigid Body Localization

Volodymyr Vizitiv[✉], Hyeon Seok Rou[✉], Niclas Führling[✉], and Giuseppe Thadeu Freitas de Abreu[✉]

School of Computer Science and Engineering, Constructor University, 28759 Bremen, Germany

[vvizitiv, hrou, nfuehring, gabreu]@constructor.university

Abstract—We propose a novel solution to the rigid body localization (RBL) problem, in which the three-dimensional (3D) rotation and translation is estimated by only utilizing the range measurements between the wireless sensors on the rigid body and the anchor sensors. Given the prior knowledge of the absolute sensor positions, by leveraging a linearized RBL transformation model with small-angle approximations, the proposed bivariate Gaussian belief propagation (GaBP) is designed to directly estimate the 3D rotation angles and translation distances, with an interference cancellation (IC) refinement step to further improve the angle estimation performance. The effectiveness of the proposed method is verified via numerical simulations, highlighting the superior performance of the proposed method against the state-of-the-art (SotA) techniques for the rotation and translation estimation performance.

Index Terms—Rigid body localization (RBL) and tracking, range-based positioning, Gaussian belief propagation (GaBP).

I. INTRODUCTION

Recent years have seen noteworthy advancements in wireless sensor technology capable of both wireless communications and environment parameter detection (*i.e.*, temperature, illuminance, electric signals), directing significant attention towards wireless sensor networks (WSNs) with the inherent implications for applications requiring monitoring and control, such as in smart factories and Internet-of-Things (IoT) [1], [2].

In many of the key WSN applications, including logistics, healthcare, and security, the accurate geographic location information of the sensors is essential, facing a unique challenge in that the sensor position is not a locally measurable instantaneous parameter. Consequently, the problem is already well-identified and extensively studied as the sensor localization problem [3], [4]. However, next-generation technologies and applications such as virtual reality (VR), extended reality (XR), robotics, and autonomous vehicles, require not only the precise location information of the sensors, but also the orientation of the sensor network associated to a given body or object [5]–[7]. This challenge has gained increasing popularity and is referred to as the rigid body localization (RBL) problem [8], [9], where the sensor network is defined as a *rigid* conformation, whose translation and rotation (*i.e.*, orientation) must be estimated for single or multiple *bodies*.

Several effective strategies have been developed to address the RBL problem, for example, computer vision-based techniques for feature extraction and posture estimation [10], [11] often requiring high volumes of image/video data and high-complexity methods involving machine learning (ML), or inertial measurement unit (IMU)-based orientation and position

estimation techniques leveraging the internal information of the accelerometers, gyroscopes, and magnetometers [12], [13] often requiring costly hardware, precise sensor calibration, and aid of external radio technology.

An alternative approach with relatively small processing requirement and simple hardware, aim to exploit the range measurements between the sensors on the rigid body and the set of *anchor* sensors of known positions [14], [15], *i.e.*, sensors on static infrastructure of the environment, which can be obtained from the time of arrival (TOA) or time difference of arrival (TDOA) data often already available from the communications functionality of the wireless sensors. In such methods, the initial estimation of the sensor position is performed with the range measurement data without the sensor conformation, followed by the extraction of the translation and rotation parameters (translation distance and rotation angles associated with each axis) subject to the rigid body constraints [16], [17]. To elaborate on a state-of-the-art (SotA) example, the method in [18] leverages the divide and conquer (DAC) approach [19] to estimate the sensor positions from the range measurements, then extracts the rotation and translation parameters via singular value decomposition (SVD)-based analysis. Finally, a conformation-based refinement based on the Euler angles formulation and weighted least squares (WLS) is performed on the obtained rotation and translation estimates.

In light of the above, we propose a novel RBL algorithm which is capable of estimating the translation distance and rotation angle from the sensor range measurements and the rigid body conformation, enabled by a linearized reformulation of the system model and a tailored design of two low-complexity Gaussian belief propagation (GaBP) [20] estimators. The proposed method is shown to outperform the SotA two-stage RBL methods in the translation and rotation estimation performance, while retaining the low computational complexity that is shown to be linear on the number of sensors.

The remainder of the article is structured as follows: Section II describes the system model and formulates the fundamental RBL estimation problem, Section II-C presents the proposed linearized reformulation leveraging small angle approximation and the RBL conformation constraints, Section III elaborates the derivation of the message passing rules for the proposed GaBP estimator for the translation and rotation parameters, and finally Section IV compares the performance of the proposed method against the SotA two-stage method [18] via numerical simulations.

II. RIGID BODY LOCALIZATION SYSTEM MODEL

A. Rigid Body System Model

Consider a scenario where a rigid body consisting of N sensors is surrounded by a total of M anchor sensors (hereafter referred simply as anchors), as illustrated in Figure 1. The sensors are described by a 3×1 vector consisting of the x, y, z -coordinates in the three-dimensional (3D) Euclidean space, denoted by $\mathbf{c}_n \in \mathbb{R}^{3 \times 1}$ for $n = \{1, \dots, N\}$ and $\mathbf{a}_m \in \mathbb{R}^{3 \times 1}$ for $m = \{1, \dots, M\}$, respectively for the rigid body sensors and anchors. The initial sensor structure in the rigid body is consequently defined by the conformation matrix $\mathbf{C} = [\mathbf{c}_1, \mathbf{c}_2, \dots, \mathbf{c}_N] \in \mathbb{R}^{3 \times N}$ at the reference frame (local axis) of the rigid body.

A transformation of the rigid body in 3D space can be fully defined by a translation and rotation, respectively described by the translation vector $\mathbf{t} \triangleq [t_x, t_y, t_z]^T \in \mathbb{R}^{3 \times 1}$ consisting of the translation distances in each axis, and a 3D rotation matrix¹ $\mathbf{Q} \in \mathbb{R}^{3 \times 3}$ given by

$$\mathbf{Q} \triangleq \begin{matrix} \triangleq \mathbf{Q}_z \in \mathbb{R}^{3 \times 3} & \triangleq \mathbf{Q}_y \in \mathbb{R}^{3 \times 3} & \triangleq \mathbf{Q}_x \in \mathbb{R}^{3 \times 3} \\ \begin{bmatrix} \cos \theta_z & -\sin \theta_z & 0 \\ \sin \theta_z & \cos \theta_z & 0 \\ 0 & 0 & 1 \end{bmatrix} \cdot \begin{bmatrix} \cos \theta_y & 0 & \sin \theta_y \\ 0 & 1 & 0 \\ -\sin \theta_y & 0 & \cos \theta_y \end{bmatrix} \cdot \begin{bmatrix} 1 & 0 & 0 \\ 0 & \cos \theta_x & -\sin \theta_x \\ 0 & \sin \theta_x & \cos \theta_x \end{bmatrix}, \end{matrix} \quad (1)$$

where $\mathbf{Q}_x, \mathbf{Q}_y, \mathbf{Q}_z \in \mathbb{R}^{3 \times 3}$ are the roll, pitch, and yaw rotation matrices about the x, y, z -axes by rotation angles of $\theta_x, \theta_y, \theta_z \in [-180^\circ, 180^\circ]$ degrees, respectively.

In light of the above, the transformed coordinates of the n -th sensor after the rotation and translation is described by

$$\mathbf{s}_n = \mathbf{Q}\mathbf{c}_n + \mathbf{t} \in \mathbb{R}^{3 \times 1}, \quad (2)$$

which is applied identically to all N sensors of the rigid body, as illustrated in Figure 2.

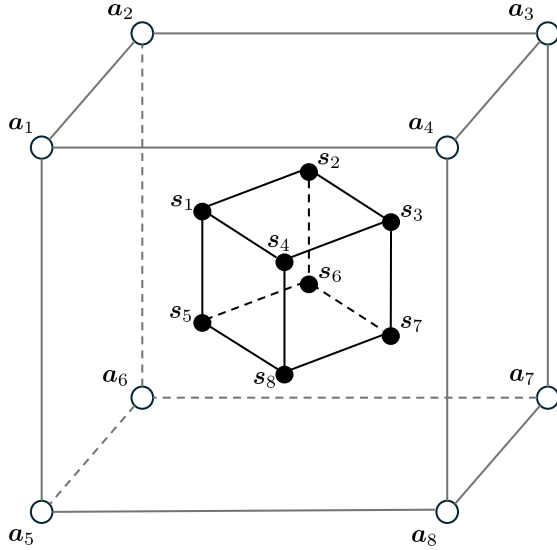


Fig. 1: An illustration of the rigid body sensor and anchor structure, exemplified by a cubic rigid body ($N = 8$) surrounded by a cubic deployment of anchors ($M = 8$).

¹The rotation matrix \mathbf{Q} is part of the special orthogonal group such that $SO(3) = \{\mathbf{Q} \in \mathbb{R}^{3 \times 3} : \mathbf{Q}^T \mathbf{Q} = \mathbf{I}, \det(\mathbf{Q}) = 1\}$ [22].

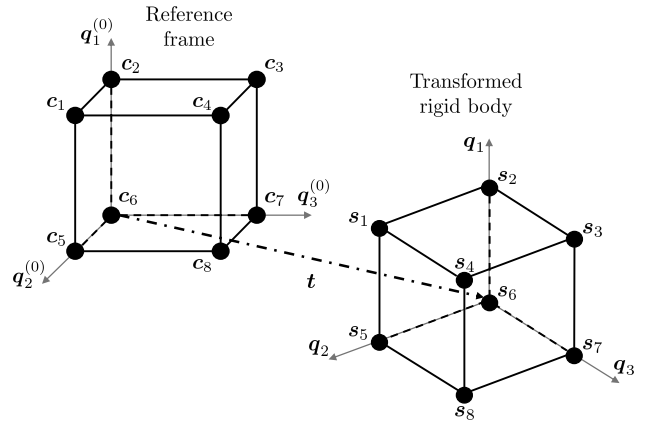


Fig. 2: An illustration of the rigid body transform composed of a 3D rotation \mathbf{Q} and translation \mathbf{t} , from the reference frame² to the transformed sensor positions determined by equation (2).

B. Position-based System Model

In this article, RBL is performed using the pairwise range measurement information between the anchors and sensors, which is assumed to be available and described by

$$\tilde{d}_{m,n} = d_{m,n} + w_{m,n} = \|\mathbf{a}_m - \mathbf{s}_n\|_2 + w_{m,n} \in \mathbb{R}, \quad (3)$$

where $d_{m,n} \triangleq \|\mathbf{a}_m - \mathbf{s}_n\|_2 \in \mathbb{R}$ is the true Euclidean distance between m -th anchor and n -th sensor, and $w_{m,n} \sim \mathcal{N}(0, \sigma_w^2)$ is the independent and identically distributed (i.i.d.) additive white Gaussian noise (AWGN) of the range measurement with noise variance σ_w^2 .

Following the above, the squared information of the range measurement is given by

$$\tilde{d}_{m,n}^2 = \|\mathbf{a}_m - \mathbf{s}_n\|_2^2 + 2d_{m,n}w_{m,n} + w_{m,n}^2 \in \mathbb{R}, \quad (4)$$

which can be reformulated as the *composite noise* $\xi_n \in \mathbb{R}$ as

$$\xi_{m,n} = \tilde{d}_{m,n}^2 - \|\mathbf{a}_m\|_2^2 - \|\mathbf{s}_n\|_2^2 + 2\mathbf{a}_m^T \mathbf{s}_n \approx 2d_{m,n}w_{m,n}, \quad (5)$$

where the second-order noise term $w_{m,n}^2$ is considered negligible and neglected [18], [23].

Stacking equation (5) for all M anchors and reformulating as a linear system on the n -th unknown sensor variable yields

$$\mathbf{y}_n \triangleq \begin{bmatrix} \tilde{d}_{1,n}^2 - \|\mathbf{a}_1\|_2^2 \\ \vdots \\ \tilde{d}_{M,n}^2 - \|\mathbf{a}_M\|_2^2 \end{bmatrix} = \underbrace{\begin{bmatrix} -2\mathbf{a}_1^T, 1 \\ \vdots \\ -2\mathbf{a}_M^T, 1 \end{bmatrix}}_{\triangleq \mathbf{G} \in \mathbb{R}^{M \times 4}} \underbrace{\begin{bmatrix} \mathbf{s}_n \\ \|\mathbf{s}_n\|_2^2 \end{bmatrix}}_{\triangleq \mathbf{x}_n \in \mathbb{R}^{4 \times 1}} + \underbrace{\begin{bmatrix} \xi_{1,n} \\ \vdots \\ \xi_{M,n} \end{bmatrix}}_{\triangleq \boldsymbol{\xi}_n \in \mathbb{R}^{M \times 1}} \in \mathbb{R}^{M \times 1}, \quad (6)$$

where $\mathbf{y}_n \in \mathbb{R}^{M \times 1}$ and $\mathbf{G} \in \mathbb{R}^{M \times 4}$ are respectively the observed data vector and effective channel matrix constructed from the measured ranges and anchor positions, $\mathbf{x}_n \in \mathbb{R}^{4 \times 1}$ is the unknown sensor position vector, and $\boldsymbol{\xi}_n \in \mathbb{R}^{M \times 1}$ is the vector of composite noise variables from equation (5).

²The reference frame $\mathbf{Q}^{(0)}$ may already be at an non-origin position, but since a rigid body rotation is only relative between the initial frame and the new orientation, the reference frame can be considered to be at the origin $\mathbf{Q}^{(0)} \triangleq \mathbf{I}_{3 \times 3}$ without loss of generality.

The linear system in equation (6) can be leveraged for the estimation of the unknown sensor coordinate vector \mathbf{s}_n and sensor position norm $\|\mathbf{s}\|_2^2$ in \mathbf{x}_n , from which equation (2) can be invoked for the translation and rotation extraction via Procrustes analysis or other classical algorithms [24].

C. Transformation Parameter-based System Model

In this section, the fundamental system of equation (6) is reformulated to express the system directly in terms of the RBL transformation parameters, *i.e.*, the 3D rotation angles $\boldsymbol{\theta} \triangleq [\theta_x, \theta_y, \theta_z]^T \in \mathbb{R}^{3 \times 1}$ and translation vector \mathbf{t} [25]. First, small-angle approximation³ [22] of the rotation matrix in equation (1) is obtained with $\cos \theta \approx 1$ and $\sin \theta \approx \theta$, as

$$\mathbf{Q} \approx \begin{bmatrix} 1 & \theta_z & -\theta_y \\ -\theta_z & 1 & \theta_x \\ \theta_y & -\theta_x & 1 \end{bmatrix} \in \mathbb{R}^{3 \times 3}, \quad (7)$$

which in turn can be vectorized into a linear system directly in terms of the Euler angles [18] as

$$\begin{aligned} \text{vec}(\mathbf{Q}) &= \boldsymbol{\gamma} + \mathbf{L}\boldsymbol{\theta} \\ &\triangleq \boldsymbol{\gamma} \in \mathbb{R}^{9 \times 1} \\ &= \underbrace{\begin{bmatrix} 1 & 0 & 0 & 0 & 1 & 0 & 0 & 0 & 1 \end{bmatrix}^T}_{\triangleq \mathbf{L} \in \mathbb{R}^{9 \times 3}} \\ &+ \underbrace{\begin{bmatrix} 0 & 1 & 0 & -1 & 0 & 0 & 0 & 0 & 0 \\ 0 & 0 & -1 & 0 & 0 & 0 & 1 & 0 & 0 \\ 0 & 0 & 0 & 0 & 0 & 1 & 0 & -1 & 0 \end{bmatrix}^T}_{\triangleq \mathbf{L} \in \mathbb{R}^{9 \times 3}} \cdot \begin{bmatrix} \theta_x \\ \theta_y \\ \theta_z \end{bmatrix} \in \mathbb{R}^{9 \times 1}. \end{aligned} \quad (8)$$

Then substituting equation (8) into equations (2) and (5) and rearranging the terms yields the alternate representation of the composite noise as

$$\begin{aligned} \xi_n &= \tilde{d}_{m,n}^2 - \|\mathbf{a}_m\|_2^2 - \|\mathbf{s}_n\|_2^2 + 2[\mathbf{c}_n^T \otimes \mathbf{a}_m^T] \boldsymbol{\gamma} \\ &+ 2[\mathbf{c}_n^T \otimes \mathbf{a}_m^T] \mathbf{L}\boldsymbol{\theta} + 2\mathbf{a}_m^T \mathbf{t} \in \mathbb{R}, \end{aligned} \quad (9)$$

where the matrix product vectorization identity $\text{vec}(\mathbf{XYZ}) = (\mathbf{Z}^T \otimes \mathbf{X})\text{vec}(\mathbf{Y})$ has been used, with Kronecker product \otimes .

In light of the above, the fundamental system can be rewritten leveraging the linearization of equation (9),

$$\mathbf{z}_n = \mathbf{H}^\theta \cdot \boldsymbol{\theta} + \mathbf{H}^t \cdot \mathbf{t} + \boldsymbol{\xi}_n \in \mathbb{R}^{M \times 1}, \quad (10a)$$

with

$$\mathbf{z}_n = \begin{bmatrix} \tilde{d}_{1,n}^2 - \|\mathbf{a}_1\|_2^2 - \|\mathbf{s}_n\|_2^2 + 2[\mathbf{c}_n^T \otimes \mathbf{a}_1^T] \boldsymbol{\gamma} \\ \vdots \\ \tilde{d}_{M,n}^2 - \|\mathbf{a}_M\|_2^2 - \|\mathbf{s}_n\|_2^2 + 2[\mathbf{c}_n^T \otimes \mathbf{a}_M^T] \boldsymbol{\gamma} \end{bmatrix} \in \mathbb{R}^{M \times 1}, \quad (10b)$$

$$\mathbf{H}^\theta = \begin{bmatrix} -2[\mathbf{c}_1^T \otimes \mathbf{a}_1^T] \mathbf{L} \\ \vdots \\ -2[\mathbf{c}_M^T \otimes \mathbf{a}_M^T] \mathbf{L} \end{bmatrix} \in \mathbb{R}^{M \times 3}, \quad \mathbf{H}^t = \begin{bmatrix} -2\mathbf{a}_1^T \\ \vdots \\ -2\mathbf{a}_M^T \end{bmatrix} \in \mathbb{R}^{M \times 3}, \quad (10c)$$

where $\mathbf{z}_n \in \mathbb{R}^{M \times 1}$ is the effective observed data vector, and $\mathbf{H}^\theta \in \mathbb{R}^{M \times 3}$ and $\mathbf{H}^t \in \mathbb{R}^{M \times 3}$ are respectively the effective channel matrices for the unknown rotation and translation variables, and $\boldsymbol{\xi}_n \in \mathbb{R}^{M \times 1}$ is the vector of composite noise variables from equation (5).

³For practical rigid body tracking applications, subsequent transformation estimations can be assumed to be performed within a sufficiently short time period, such that the change in rotation angle is small.

III. PROPOSED RBL METHOD

In light of the system model derived in Section II, a low-complexity transformation parameter estimator for RBL is proposed by a tailored message passing algorithm under the GaBP framework. Given the absolute sensor coordinate information obtained by solving the position-explicit system in equation (6) using existing methods such as closed-form two-stage method [21] or any other SotA range-based technique, a proper GaBP is derived on the rigid body transformation parameter-explicit system in equation (10), to obtain the final estimate of the rotation angle $\boldsymbol{\theta}$ and translation \mathbf{t} .

A. Bivariate GaBP for Transformation Parameter Estimation

Remark: As the GaBP derivation for each n -th linear system corresponding to the n -th sensor node $\forall n \in \{1, \dots, N\}$ are identical, the subscript n is omitted from onwards.

As can be seen in the reformulated system of the transformation parameter estimation in equation (10a), there exist two sets of variables θ_k with $k \in \{1, \dots, K\}$ and t_ℓ with $\ell \in \{1, \dots, K\}$, whose soft-replicas of the k -th, ℓ -th elements via the m -th observation is denoted by $\hat{\theta}_{m,k}^{[\lambda]}$, $\hat{t}_{m,\ell}^{[\lambda]}$, respectively.

Firstly, the soft-interference cancellation (IC) is performed on the observed information respectively for the angle and translation variables as

$$\tilde{z}_{m,k}^{\theta[\lambda]} = z_m - \sum_{i \neq k} h_{m,i}^\theta \hat{\theta}_{m,i}^{[\lambda]} - \sum_{i=1}^K h_{m,i}^t \hat{t}_{m,i}^{[\lambda]}, \quad (11a)$$

$$= h_{m,k}^\theta \theta_k + \sum_{i \neq k} h_{m,i}^\theta (\theta_i - \hat{\theta}_{m,i}^{[\lambda]}) + \sum_{i=1}^K h_{m,i}^t (t_i - \hat{t}_{m,i}^{[\lambda]}) + \xi_m,$$

$$\tilde{z}_{m,\ell}^{t[\lambda]} = z_m - \sum_{i=1}^K h_{m,i}^\theta \hat{\theta}_{m,i}^{[\lambda]} - \sum_{i \neq \ell} h_{m,i}^t \hat{t}_{m,i}^{[\lambda]}, \quad (11b)$$

$$= h_{m,\ell}^t t_\ell + \sum_{i=1}^K h_{m,i}^\theta (\theta_i - \hat{\theta}_{m,i}^{[\lambda]}) + \sum_{i \neq \ell} h_{m,i}^t (t_i - \hat{t}_{m,i}^{[\lambda]}) + \xi_m.$$

In turn, the conditional probability density functions (PDFs) of the soft-IC symbols are given by

$$\begin{aligned} p_{\tilde{z}_{m,k}^{\theta[\lambda]} | \theta_k}(\tilde{z}_{m,k}^{\theta[\lambda]} | \theta_k) &\propto \exp \left[-\frac{|\tilde{z}_{m,k}^{\theta[\lambda]} - h_{m,k}^\theta \theta_k|^2}{(\sigma_{m,k}^{\theta[\lambda]})^2} \right], \\ p_{\tilde{z}_{m,\ell}^{t[\lambda]} | t_\ell}(\tilde{z}_{m,\ell}^{t[\lambda]} | t_\ell) &\propto \exp \left[-\frac{|\tilde{z}_{m,\ell}^{t[\lambda]} - h_{m,\ell}^t t_\ell|^2}{(\sigma_{m,\ell}^{t[\lambda]})^2} \right], \end{aligned} \quad (12)$$

with conditional variances

$$(\sigma_{m,k}^{\theta[\lambda]})^2 = \sum_{i \neq k} |h_{m,i}^\theta|^2 \psi_{m,i}^{\theta[\lambda]} + \sum_{i=1}^K |h_{m,i}^t|^2 \psi_{m,i}^{t[\lambda]} + N_0 \in \mathbb{R}, \quad (13a)$$

$$(\sigma_{m,\ell}^{t[\lambda]})^2 = \sum_{i=1}^K |h_{m,i}^\theta|^2 \psi_{m,i}^{\theta[\lambda]} + \sum_{i \neq \ell} |h_{m,i}^t|^2 \psi_{m,i}^{t[\lambda]} + N_0 \in \mathbb{R}, \quad (13b)$$

where $\psi_{m,k}^{\theta[\lambda]} = \mathbb{E}_{\theta_k} [|\theta_k - \hat{\theta}_{m,k}^{[\lambda]}|^2]$, $\psi_{m,\ell}^{t[\lambda]} = \mathbb{E}_{t_\ell} [|t_\ell - \hat{t}_{m,\ell}^{[\lambda]}|^2]$ are the corresponding mean-squared-errors (MSEs).

In hand of the conditional PDFs, the extrinsic PDF is obtained as

$$\prod_{i \neq m} p_{\tilde{z}_{i,k}^{\theta[\lambda]} | \theta_k} \left(\tilde{z}_{i,k}^{\theta[\lambda]} | \theta_k \right) \propto \exp \left[-\frac{|\theta_k - \bar{\theta}_{m,k}^{\theta[\lambda]}|^2}{\bar{v}_{m,k}^{\theta[\lambda]}} \right], \quad (14)$$

$$\prod_{i \neq m} p_{\tilde{z}_{i,\ell}^{t[\lambda]} | t_\ell} \left(\tilde{z}_{i,\ell}^{t[\lambda]} | t_\ell \right) \propto \exp \left[-\frac{|t_\ell - \bar{t}_{m,\ell}^{t[\lambda]}|^2}{\bar{v}_{m,\ell}^{t[\lambda]}} \right],$$

where the corresponding extrinsic means and variances are defined as

$$\bar{\theta}_{m,k}^{\theta[\lambda]} = \bar{v}_{m,k}^{\theta[\lambda]} \left(\sum_{i \neq m} \frac{h_{i,k}^{\theta} \cdot \tilde{z}_{i,k}^{\theta[\lambda]}}{(\sigma_{i,k}^{\theta[\lambda]})^2} \right) \in \mathbb{R}, \quad (15a)$$

$$\bar{t}_{m,\ell}^{t[\lambda]} = \bar{v}_{m,\ell}^{t[\lambda]} \left(\sum_{i \neq m} \frac{h_{i,\ell}^t \cdot \tilde{z}_{i,\ell}^{t[\lambda]}}{(\sigma_{i,\ell}^{t[\lambda]})^2} \right) \in \mathbb{R}, \quad (15b)$$

$$\bar{v}_{m,k}^{\theta[\lambda]} = \left(\sum_{i \neq m} \frac{|h_{i,k}^{\theta}|^2}{(\sigma_{i,k}^{\theta[\lambda]})^2} \right)^{-1} \in \mathbb{R}, \quad (16a)$$

$$\bar{v}_{m,\ell}^{t[\lambda]} = \left(\sum_{i \neq m} \frac{|h_{i,\ell}^t|^2}{(\sigma_{i,\ell}^{t[\lambda]})^2} \right)^{-1} \in \mathbb{R}. \quad (16b)$$

Then, the extrinsic means and variances are denoised with a Gaussian⁴ prior to yield the new soft-replicas and MSEs, as

$$\check{\theta}_{m,k} = \frac{\phi^\theta \cdot \bar{\theta}_{m,k}^{\theta[\lambda]}}{\phi^\theta + \bar{v}_{m,k}^{\theta[\lambda]}} \in \mathbb{R}, \quad \check{t}_{m,\ell} = \frac{\phi^t \cdot \bar{t}_{m,\ell}^{t[\lambda]}}{\phi^t + \bar{v}_{m,\ell}^{t[\lambda]}} \in \mathbb{R}, \quad (17a)$$

$$\check{\psi}_{m,k}^\theta = \frac{\phi^\theta \cdot \bar{v}_{m,k}^{\theta[\lambda]}}{\phi^\theta + \bar{v}_{m,k}^{\theta[\lambda]}} \in \mathbb{R}, \quad \check{\psi}_{m,\ell}^t = \frac{\phi^t \cdot \bar{v}_{m,\ell}^{t[\lambda]}}{\phi^t + \bar{v}_{m,\ell}^{t[\lambda]}} \in \mathbb{R}, \quad (17b)$$

where ϕ^θ and ϕ^t are the variance of the elements in θ and t .

Finally, the newly computed soft-replicas and MSEs are updated via damping to prevent early erroneous convergence to a local optima and error floor, which is described by

$$\hat{\theta}_{m,k}^{[\lambda+1]} = \rho \hat{\theta}_{m,k}^{[\lambda]} + (1 - \rho) \check{\theta}_{m,k}^{[\lambda]}, \quad (18a)$$

$$\hat{t}_{m,\ell}^{[\lambda+1]} = \rho \hat{t}_{m,\ell}^{[\lambda]} + (1 - \rho) \check{t}_{m,\ell}^{[\lambda]},$$

$$\psi_{m,k}^{\theta[\lambda+1]} = \rho \psi_{m,k}^{\theta[\lambda]} + (1 - \rho) \check{\psi}_{m,k}^{\theta[\lambda]}, \quad (18b)$$

$$\psi_{m,\ell}^{t[\lambda+1]} = \rho \psi_{m,\ell}^{t[\lambda]} + (1 - \rho) \check{\psi}_{m,\ell}^{t[\lambda]},$$

where $\rho \in [0, 1]$ is the damping hyperparameter, and the superscript $(\cdot)^{[\lambda]}$ denotes the iterate at the λ -th GaBP iteration.

After λ_{\max} iterations of the GaBP (or some convergence criteria), the final consensus estimates of the rotation and translation parameters are obtained as

$$\tilde{\theta}_k = \left(\sum_{m=1}^M \frac{|h_{m,k}^{\theta}|^2}{(\sigma_{m,k}^{\theta[\lambda_{\max}]})^2} \right)^{-1} \left(\sum_{m=1}^M \frac{h_{m,k}^{\theta} \cdot \tilde{z}_{m,k}^{\theta[\lambda_{\max}]}}{(\sigma_{m,k}^{\theta[\lambda_{\max}]})^2} \right) \in \mathbb{R}, \quad (19a)$$

$$\tilde{t}_\ell = \left(\sum_{m=1}^M \frac{|h_{m,\ell}^t|^2}{(\sigma_{m,\ell}^{t[\lambda_{\max}]})^2} \right)^{-1} \left(\sum_{m=1}^M \frac{h_{m,\ell}^t \cdot \tilde{z}_{m,\ell}^{t[\lambda_{\max}]}}{(\sigma_{m,\ell}^{t[\lambda_{\max}]})^2} \right) \in \mathbb{R}. \quad (19b)$$

⁴If an alternative prior distribution of the position variables are assumed, i.e., uniform distribution, a different Bayes-optimal denoiser can be utilized.

While the message passing rules elaborated are complete to yield the estimated rotation angles and translation vectors, due to the effective channel powers of \mathbf{H}^θ and \mathbf{H}^t in equation (10) where the latter is typically much larger absolute positions of the anchors and sensors⁵. Such significant difference in effective channel powers lead to good estimation performance of the translation vector elements, but erroneous estimation performance of the rotation angles in a joint estimation described by the GaBP procedure.

This behavior can also be intuitively understood by considering the illustration in Figure 2, where the rotation of the rigid body is expected to have a less prominent effect on the absolute sensor positions compared to the effect of the translation when the rotation angles are not too large, as assumed in the system formulation of Section II.

Then, in order to address the aforementioned error behavior of the rotation angle parameters θ , we propose an interference cancellation-based approach to remove the components corresponding to the translation of the sensors, and perform the GaBP again only on the rotation angle parameters. Namely, by using the estimated consensus translation vector $\tilde{\mathbf{t}} \triangleq [\tilde{t}_1, \tilde{t}_2, \tilde{t}_3]^T \in \mathbb{R}^{3 \times 1}$ obtained at the end of the GaBP via equation (19b), the interference-cancelled system is given by

$$\mathbf{z}'_n \triangleq \mathbf{z}_n - \mathbf{H}^t \tilde{\mathbf{t}} = \mathbf{H}^\theta \theta + \xi_n \in \mathbb{R}^{M \times 1}. \quad (20)$$

Algorithm 1 : Double GaBP for RBL Parameter Estimation

Input: \mathbf{z}_n ($\|\mathbf{s}_n\|_2^2 \forall n$), \mathbf{H}^θ , \mathbf{H}^t , ϕ^θ , ϕ^t , N_0 , λ_{\max} , ρ .

Output: θ_k and $t_\ell \forall k, \ell$ (for all sensor nodes $\forall n$);

Perform $\forall n, m, k, \ell$:

- 1: Initialise $\hat{\theta}_{m,k}^{[1]}$, $\hat{t}_{m,\ell}^{[1]}$, $\psi_{m,k}^{\theta[1]}$, $\psi_{m,\ell}^{t[1]}$.
 - 2: **for** $\lambda = 1$ to λ_{\max} **do**
 - 3: Compute soft-IC symbols $\tilde{z}_{m,k}^{\theta[\lambda]}$, $\tilde{z}_{m,\ell}^{t[\lambda]}$ via eq. (11);
 - 4: Compute cond. variances $(\sigma_{m,k}^{\theta[\lambda]})^2$, $(\sigma_{m,\ell}^{t[\lambda]})^2$ via eq. (13);
 - 5: Compute extrinsic means $\bar{\theta}_{m,k}^{\theta[\lambda]}$, $\bar{t}_{m,\ell}^{t[\lambda]}$ via eq. (15);
 - 6: Compute extrinsic variances $\bar{v}_{m,k}^{\theta[\lambda]}$, $\bar{v}_{m,\ell}^{t[\lambda]}$ via eq. (16);
 - 7: Denoise the beliefs $\check{\theta}_{m,k}$, $\check{t}_{m,\ell}$ via eq. (17a);
 - 8: Denoise the error variances $\check{\psi}_{m,k}^\theta$, $\check{\psi}_{m,\ell}^t$ via eq. (17b);
 - 9: Update the soft-replicas with damping as in eq. (18);
 - 10: **end for**
 - 11: Obtain final consensus estimates $\tilde{\theta}_k$, \tilde{t}_ℓ via eq. (19);
 - 12: Obtain interference-cancelled system via eq. (20);
 - 13: **for** $\lambda = 1$ to λ_{\max} **do**
 - 14: Compute soft-IC symbols $\tilde{z}'_{m,k}^{\theta[\lambda]}$ via eq. (21);
 - 15: Compute conditional variances $(\sigma_{m,k}^{\theta[\lambda]})^2$ via eq. (22);
 - 16: Compute extrinsic means $\bar{\theta}_{m,k}^{\theta[\lambda]}$ via eq. (15a);
 - 17: Compute extrinsic variances $\bar{v}_{m,k}^{\theta[\lambda]}$ via eq. (16a);
 - 18: Denoise the beliefs $\check{\theta}_{m,k}$ via eq. (17a);
 - 19: Denoise the error variances $\check{\psi}_{m,k}^\theta$ via eq. (17b);
 - 20: Update the soft-replicas with damping as in eq. (18);
 - 21: **end for**
 - 22: Obtain refined consensus estimates $\tilde{\theta}_k$ via eq. (19a);
-

⁵The effective channel powers are highly dependent on the sensor and anchor deployment structure, and for typical indoor sensing scenarios as illustrated in Figure 1, the anchor coordinates are of larger absolute value than the rigid body sensor coordinates, leading to the large power difference.

The second GaBP procedure to estimate the rotation angles θ is identical to the message passing rules provided for θ in equations (11)-(19), after an IC procedure to remove the effect of t from the system to change the message construction rules at the factor nodes for soft-IC and conditional variance computations of equations (11) and (13) into

$$\tilde{z}_{m,k}^{\theta[\lambda]} = z'_m - \sum_{i \neq k} h_{m,i}^\theta \hat{\theta}_{m,i}^{[\lambda]} \in \mathbb{R}, \quad (21)$$

$$(\sigma_{m,k}^{\theta[\lambda]})^2 = \sum_{i \neq k} |h_{m,i}^\theta|^2 \psi_{m,i}^{\theta[\lambda]} + N_0 \in \mathbb{R}, \quad (22)$$

while the remaining message passing rules on θ by the variable nodes remain the same.

The resultant single-variable GaBP on θ is concatenated with the previous bivariate GaBP to describe the complete estimation process of the rigid body transformation parameters θ and t , as summarized by Algorithm 1.

IV. PERFORMANCE ANALYSIS

In this section, we present the simulation results to demonstrate effectiveness of the proposed bivariate GaBP and interference cancellation-based refinement GaBP concatenated in Algorithm 1 for RBL, directly in terms of the rotation and translation parameter estimation performance. The performance is compared against the relevant SotA RBL solution, whose initial TOA-based sensor position estimation is performed via the approach in [21] and the consequent RBL parameter estimation proposed in [18], which is performed via WLS-based closed-form two-stage method, incorporating a DAC approach. Therefore, for a fair comparison, the initial sensor position information required for our proposed approach is also provided by the same SotA TOA-based method [21], whose details has not been included in this article due to page limitations.

The simulation setup is the scenario illustrated in Figure 1, where the rigid body is composed of $N = 8$ sensors positioned at the vertices of a unit cube at the origin, with sensor positions described by the conformation matrix given by

$$\mathbf{C} = \begin{bmatrix} -0.5 & 0.5 & 0.5 & -0.5 & -0.5 & 0.5 & -0.5 & 0.5 \\ -0.5 & -0.5 & 0.5 & 0.5 & -0.5 & -0.5 & 0.5 & 0.5 \\ -0.5 & -0.5 & -0.5 & -0.5 & 0.5 & 0.5 & 0.5 & 0.5 \end{bmatrix} \in \mathbb{R}^{3 \times 8},$$

and the $M = 8$ anchors are positioned at the vertices of a larger cube (*i.e.*, an indoor scenario at the corners of the room), where the anchor conformation matrix $\mathbf{A} \in \mathbb{R}^{3 \times 8}$ is given by

$$\mathbf{A} = \begin{bmatrix} -10 & 10 & 10 & -10 & -10 & 10 & -10 & 10 \\ -10 & -10 & 10 & 10 & -10 & -10 & 10 & 10 \\ -10 & -10 & -10 & -10 & 10 & 10 & 10 & 10 \end{bmatrix} \in \mathbb{R}^{3 \times 8}.$$

The RBL rotation angles $\theta_x, \theta_y, \theta_z$ follow a zero-mean Gaussian distribution of variance $\phi^\theta = 10$, and the RBL translation vector elements also follow a zero-mean Gaussian distribution of variance $\phi^t = 5$.

The performance is assessed using the root-mean-squared-error (RMSE) defined as

$$\text{RMSE} = \sqrt{\frac{1}{E} \sum_{j=1}^E \|\hat{\mathbf{x}}^{[j]} - \mathbf{x}\|_2^2}, \quad (23)$$

where $\hat{\mathbf{x}}^{[j]}$ is the RBL parameter vector (position, angle, or translation) estimated during the j -th Monte-Carlo simulation, \mathbf{x} is the true RBL parameter vector, and $E = 10^3$ is the total number of independent Monte-Carlo experiments used for the analysis, and is evaluated for different noise standard deviations σ of equation (3), a.k.a. the range error in meters.

The estimation performances of the rigid body translation parameters and rotation angle parameters have been illustrated in Figures 3 and 4, respectively.

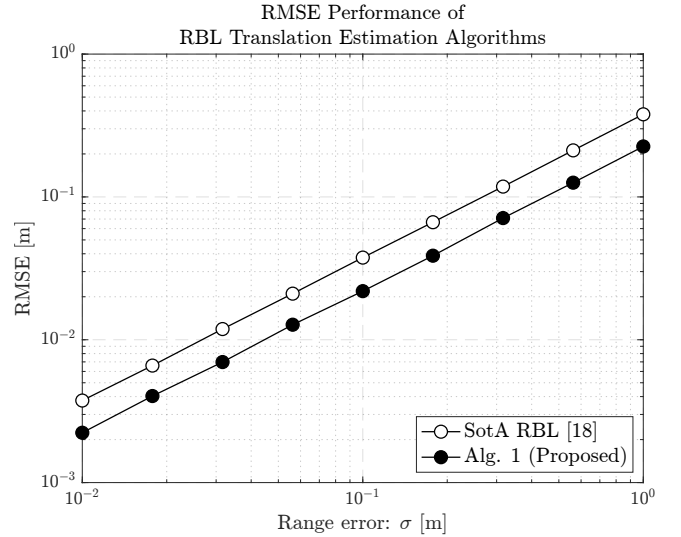


Fig. 3: RMSE of the proposed bivariate GaBP algorithm for rigid body translation parameter estimation (Alg. 1) and the SotA method of [18], for various range errors σ .

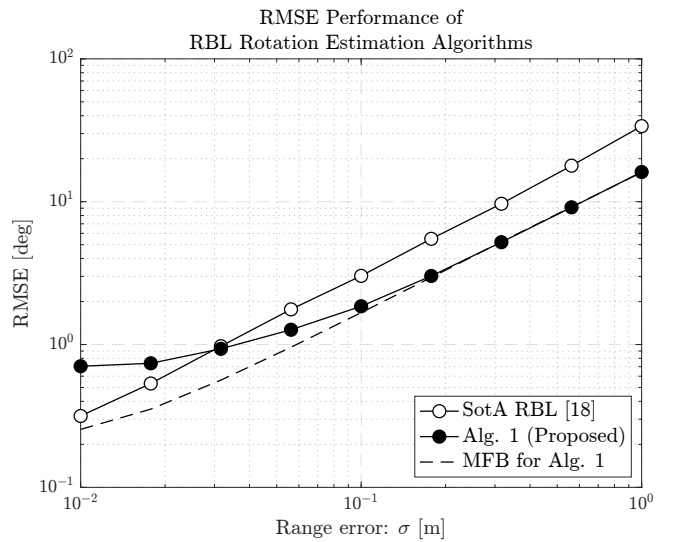


Fig. 4: RMSE of the proposed bivariate GaBP algorithm for rigid body rotation angle parameter estimation (Alg. 1) and the SotA method of [18], for various range errors σ .

As mentioned in Section III, the translation parameter can be effectively estimated via the proposed bivariate GaBP of Algorithm 1 in light of the channel power difference effect, which is highlighted by the result of Figure 3. It can be seen that the proposed bivariate GaBP algorithm outperforms the SVD-based SotA approach [18] in terms of the rotation angle estimation, for all regimes of range error.

Finally, Figure 4 illustrates the estimation performance of the rotation angles of the rigid body transformation. It can be observed that the estimation performance of the proposed concatenated GaBP also exhibits superiority to the SotA method, similarly to the behavior of the translation estimation performance. However, due to the aforementioned channel power scaling effect which causes the noise power to be more prominent in the estimation of the variables, the GaBP is shown to exhibit an error floor for small range error regimes. Various methods exist to mitigate the error-floors [26], [27], which are well-identified for message passing algorithms under non-ideal conditions, whose incorporation and extension is considered out of scope of this article. Instead, the ideal behavior of the proposed algorithm is illustrated via the matched filter bound (MFB) of the GaBP algorithm, which shows the expected superiority over all noise ranges.

V. CONCLUSION

We presented a novel and efficient technique for solving the RBL problem directly in terms of the 3D rotation and translation parameters from known sensor positions, via a series of tailored GaBP message passing estimators. The RBL system is first reformulated via the small-angle approximation to enable the construction of a bivariate GaBP which is capable of directly estimating the rotation angles and the translation distances. Then, a second interference cancellation-based second GaBP to improve the performance of the rotation angle parameter estimation is incorporated, to mitigate the effect of imbalanced effective channel powers of the bivariate system. The proposed concatenated GaBP-based RBL method is shown to outperform the SotA method in both the rotation and translation estimation performance, except for the appearance of an error-floor for the rotation angle estimation at low range error regimes. Future works will aim to address the mitigation of such error-floor, enhanced robustness under diverse and non-ideal conditions of sensor deployment and conformations, via matrix completion and advanced belief propagation techniques.

REFERENCES

- [1] M. A. Jamshed *et al.*, "Challenges, Applications, and Future of Wireless Sensors in Internet of Things: A review," *IEEE Sensors Journal*, vol. 22, no. 6, pp. 5482–5494, 2022.
- [2] D. Kandris, C. Nakas, D. Vomvas, and G. Koulouras, "Applications of Wireless Sensor Networks: an up-to-date survey," *Applied System Innovation*, vol. 3, no. 1, p. 14, 2020.
- [3] N. Patwari *et al.*, "Locating the Nodes: Cooperative Localization in Wireless Sensor Networks," *IEEE Signal Processing Magazine*, vol. 22, no. 4, pp. 54–69, 2005.
- [4] F. Gustafsson and F. Gunnarsson, "Mobile Positioning using Wireless Networks: Possibilities and Fundamental Limitations Based on Available Wireless Network Measurements," *IEEE Signal Processing Magazine*, vol. 22, no. 4, pp. 41–53, 2005.
- [5] T.-L. Yang *et al.*, "Position and Orientation Characteristic Equation for Topological Design of Robot Mechanisms," *Journal of Mechanical Design*, vol. 131, no. 2, p. 021001, 12 2008.
- [6] J. Lee, S. C. Ahn, and J.-I. Hwang, "A Walking-in-place Method for Virtual Reality Using Position and Orientation Tracking," *Sensors*, vol. 18, no. 9, p. 2832, 2018.
- [7] W. Whittaker, "Utilization of Position and Orientation Data for Preplanning and Real Time Autonomous Vehicle Navigation," in *Proceedings of IEEE/ION PLANS 2006*, 2006, pp. 372–377.
- [8] S. P. Chepuri, G. Leus, and A.-J. van der Veen, "Rigid Body Localization using Sensor Networks," *IEEE Transactions on Signal Processing*, vol. 62, no. 18, pp. 4911–4924, 2014.
- [9] Q. Yu, Y. Wang, Y. Shen, and X. Shi, "Cooperative Multi-rigid-body Localization in Wireless Sensor Networks using Range and Doppler Measurements," *IEEE Internet of Things Journal*, 2023.
- [10] W. Chaoyi *et al.*, "Fine-grained Pose Temporal Memory Module for Video Pose Estimation and Tracking," in *ICASSP 2021-2021 IEEE International Conference on Acoustics, Speech and Signal Processing (ICASSP)*. IEEE, 2021, pp. 2205–2209.
- [11] Y. Xiang, T. Schmidt, V. Narayanan, and D. Fox, "POSECNN: A Convolutional Neural Network for 6D Object Pose Estimation in Cluttered Scenes," *arXiv preprint arXiv:1711.00199*, 2017.
- [12] F. Aghili and A. Salerno, "Driftless 3-D Attitude Determination and Positioning of Mobile Robots By Integration of IMU With Two RTK GPSS," *IEEE Trans. Mechatronics*, vol. 18, no. 1, pp. 21–31, 2013.
- [13] J. Zhao, "A Review of Wearable IMU (inertial-measurement-unit)-based Pose Estimation and Drift Reduction Technologies," in *Journal of Physics: Conference Series*, vol. 1087. IOP Publishing, 2018, pp. 042003.
- [14] A. Alcocer, P. Oliveira, A. Pascoal, R. Cunha, and C. Silvestre, "A Dynamic Estimator on SE(3) using Range-Only Measurements," in *2008 47th IEEE Conference on Decision and Control*, 2008, pp. 2302–2307.
- [15] S. Sand, A. Dammann, and C. Mensing, *Positioning in Wireless Communications Systems*, 1st ed. Wiley Publishing, 2014.
- [16] A. Beck, P. Stoica, and J. Li, "Exact and Approximate Solutions of Source Localization Problems," *IEEE Transactions on Signal Processing*, vol. 56, no. 5, pp. 1770–1778, 2008.
- [17] Y. Chan and K. Ho, "A Simple and Efficient Estimator for Hyperbolic Location," *IEEE Trans. Sig. Proc.*, vol. 42, no. 8, pp. 1905–1915, 1994.
- [18] S. Chen and K. C. Ho, "Accurate Localization of a Rigid Body Using Multiple Sensors and Landmarks," *IEEE Transactions on Signal Processing*, vol. 63, no. 24, pp. 6459–6472, 2015.
- [19] J. Abel, "A Divide and Conquer Approach to Least-Squares Estimation," *IEEE Transactions on Aerospace and Electronic Systems*, vol. 26, no. 2, pp. 423–427, 1990.
- [20] D. Bickson, "Gaussian Belief Propagation: Theory and Application," 2009.
- [21] Z. Ma and K. Ho, "TOA Localization in the Presence of Random Sensor Position Errors," in *2011 IEEE International Conference on Acoustics, Speech and Signal Processing (ICASSP)*, 2011, pp. 2468–2471.
- [22] J. Diebel, "Representing Attitude: Euler Angles, Unit Quaternions, and Rotation Vectors," *Matrix*, vol. 58, no. 15-16, pp. 1–35, 2006.
- [23] K. Ho and W. Xu, "An Accurate Algebraic Solution for Moving Source Location using TDOA and FDOA Measurements," *IEEE Transactions on Signal Processing*, vol. 52, no. 9, pp. 2453–2463, 2004.
- [24] D. W. Eggert, A. Lorusso, and R. B. Fisher, "Estimating 3-D Rigid Body Transformations: a Comparison of Four Major Algorithms," *Machine Vision and Applications*, vol. 9, no. 5, pp. 272–290, 1997.
- [25] L. Zha, D. Chen, and G. Yang, "3D Moving Rigid Body Localization in the Presence of Anchor Position Errors," 07 2021, pp. 28–32.
- [26] B. Li, N. Wu, and Y.-C. Wu, "Distributed Inference With Variational Message Passing in Gaussian Graphical Models: Tradeoffs in Message Schedules and Convergence Conditions," *IEEE Transactions on Signal Processing*, vol. 72, pp. 2021–2035, 2024.
- [27] T. Takahashi *et al.*, "Design of Adaptively Scaled Belief in Multi-dimensional Signal Detection for Higher-order Modulation," *IEEE Transactions on Communications*, vol. 67, no. 3, pp. 1986–2001, 2018.